APPENDIX 1

UPPER BOUND ANALYSIS OF DIE POWER

In continuous extrusion process considerable friction exists between the feedstock and the bore of the abutment chamber. The deformation of feedstock in abutment chamber in continuous extrusion is similar to container in conventional extrusion process. In conventional extrusion this frictional force, which opposes the motion of the ram, is a maximum at the start of the process when the feedstock is at its maximum length and reduce as the feedstock is extruded the die. The magnitude of this force is such as to limit the initial length/diameter ratio of the feedstock to about 5:1.

The unlubricated flat die produces an intensely deforming shear surface, which separates the deforming zone from the dead metal zone. The shear surface itself acts as a shaped die, but it has very high friction. So, the flat die requires a higher extrusion power. Also the extrusion speed is limited due to hot shortness. Shaped extrusion dies can overcome these difficulties. But they are difficult to design and manufacture. However, with the advent of computers in design and manufacture, these difficulties have been diminished.

Based on the kinematically admissible velocity field, an upper bound solution obtained by [Gunasekera and Hoshino, (1982)], [Gunasekera and Hoshino, (1985)] for the regular polygonal sections is modified here to suit the kinematic velocity field requirements for general shapes. [Kumar et al., (1999)], [Kumar et al., (2002)] used a fourth order polynomial to obtain the kinematically admissible velocity field in terms of stream function for generalized shapes.

CONSTITUTIVE EQUATIONS

The system of equations describing the behavior of solid various types of response is referred to as the constitutive equations. In steady-state forming processes such as extrusion, drawing, rolling, etc. the measure of deformation is the strain rate tensor $\in_{ij}$, which is expressed as

$$\in_{ij} = \frac{1}{2}\left(\frac{\partial v_i}{\partial x_j} + \frac{\partial v_j}{\partial x_i}\right) \tag{1.1}$$

Where v_i and v_j represent the velocity components along x_i and x_j direction respectively. In order to express the constitutive equation in a convenient the stress tensor σ_{ij} is decomposed as

$$\sigma_{ij} = -p\delta_{ij} + \sigma_{ij}^{'}$$

$$p = -\frac{\sigma_{kk}}{3}$$

Where p is the hydrostatic part, δ_{ij} is Kronecker's delta and $\sigma_{ij}^{'}$ is the deviatoric part of the total stress σ_{ij}

In bulk metal forming processes such as extrusion, drawing, rolling, etc. the total strains are large as compared to the elastic strains. Therefore elastic deformation can be considered as negligible compared to plastic/viscoplastic deformation. The constitutive law for rigid plastic/viscoplastic material relating the deviatoric stress tensor $\sigma_{ij}^{'}$ and the strain rate tensor $\dot{\epsilon}_{ij}$ is expressed as

$$\sigma_{ij}^{'} = 2\mu\,\dot{\epsilon}_{ij} \tag{1.2}$$

For a material yielding according to Von-Mises criterion, the Levy-Mises coefficient μ is given by

$$\mu = \frac{\overline{\sigma}}{3\,\dot{\overline{\epsilon}}} \tag{1.3}$$

Where the generalized yield stress $\overline{\sigma}$ and the generalized strain rate $\dot{\overline{\epsilon}}$ are defined as

$$\overline{\sigma} = \sqrt{\frac{3}{2}\sigma_{ij}^{'}\sigma_{ij}^{'}} \tag{1.4}$$

and $\quad \dot{\overline{\epsilon}} = \sqrt{\frac{2}{3}\dot{\epsilon}_{ij}\,\dot{\epsilon}_{ij}} \tag{1.5}$

The generalized strain $\overline{\epsilon}$ is therefore, defined as

$$\overline{\epsilon} = \int_0^t \dot{\overline{\epsilon}}\,dt \tag{1.6}$$

Where the integration is to be carried along the particle path.

In general $\overline{\sigma}$ depends on $\overline{\epsilon}, \dot{\overline{\epsilon}}$ and temperature T.

287

$$\bar{\sigma} = F(\bar{\epsilon}, \dot{\bar{\epsilon}}, T) \tag{1.7}$$

In case of cold extrusion the effect of temperature can be neglected on generalized stress $\bar{\sigma}$. The specific functional form of F for the material under consideration is mentioned at respective places. The above equations are used in the proposed upper bound solution.

UPPER BOUND FORMULATION

General Methodology

An upper bound solution is required to satisfy only the kinematic conditions in terms of strain increments, strain rate and velocities in a plastically deforming medium and does not necessarily satisfy the stress equilibrium equations. An important concept involved is that of a kinematically admissible velocity field. Velocity fields that satisfy the constraint of volume constancy and the velocity boundary conditions are called kinematically admissible velocity fields. A kinematically admissible velocity field may have discontinuities in the tangential component along certain surfaces, but the normal component must be the same on both sides of such surfaces in order to satisfy the constraint of incompressibility. The unknown parameters in kinematically admissible velocity field are determined using the upper bound solution.

The upper bound theorem [Prager and Hodge, 1951] states that among all possible kinematically admissible velocity fields, the one that minimizes the total power φ_T is the actual velocity field.

$$\varphi_T = \int_{\Omega} \sigma_{ij}^* \dot{\epsilon}_{ij}^* \, d\Omega + \int_{S_i} \tau |\Delta v_i|_{S_i}^* \, dS_i \tag{1.8}$$

In the above equation Ω is the plastic deformation zone, τ is the shear stress on velocity discontinuity surfaces S_i (Figure 1.1)
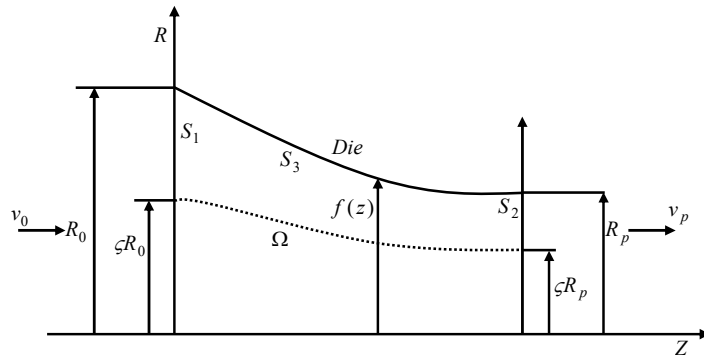

Figure 1.1: Deformation zone and typical stream surfaces in extrusion

S_1 – Entry

Surface S_2 – Exit Surface S_3 – Feedstock Interface

The first term expresses the internal power of deformation over the volume of the deformation zone, while the second term represents the power dissipated in shearing the material over the velocity discontinuity surfaces and at the tool-work interface (i.e. frictional power), Here asterisk (*) indicates that the values of stress, strain rate and velocity discontinuity are obtained from an assumed kinematically admissible velocity field.

Deformation Zone and Velocity Boundary Conditions

In most of the earlier works on upper bound method, a lot of emphasis was given to the determination of complex shapes of plastic boundaries S_1 and S_2 shown in Figure 3.1. The predictions of these boundaries are never accurate since the upper bound analysis does not satisfy stress equilibrium. The upper bound solution obtained by earlier researchers using straight and arbitrarily shaped plastic boundaries indicate that there is little effect of the shapes of surfaces S_1 and S_2 on the overall solution. Hence, in the present work, the deformation zone Ω is assumed to be bounded by straight plastic boundaries at the end sections of the die. This assumption simplifies the mathematical treatment of the problem significantly without compromising much on accuracy and provides greater flexibility in the optimization of the die profile S_3. Material is assumed to be rigid outside the entry and exit sections of the die. Therefore, the axial velocity at the entry and exit sections of the die should be uniform. These conditions are given by:

$$v_z = v_o \qquad \text{on } S_1$$

$$v_z = v_o \qquad\qquad\qquad\qquad\qquad\qquad\qquad \text{on } S_2$$
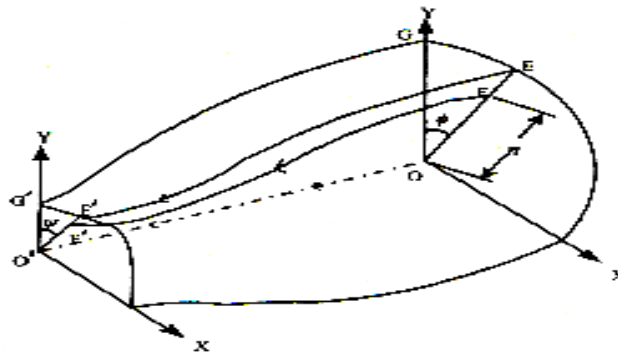
$$\text{(1.9)}$$

Figure 1.2: Geometry of die and stream lines in an extrusion die

At cross-section S_2 different points have different velocities. A point at the centre has maximum velocity and a point on the periphery has minimum velocity. Corresponding to N different points, the common velocity of extrudate v_p is defined as

$$v_p = \left(\sum_{i=1}^{i=N} v_i \right) / N \qquad (1.10)$$

There should not be any metal flow across boundary S_3 and the axis of symmetry. This condition on these boundaries can be expressed as

$$v_n = 0 \qquad (1.11)$$

on die surface S_3 and the axis of symmetry.

Estimation of Extrusion Power and Average Ram Pressure

The total power consumed inside the die is the sum of total power consumed within different power elements. One such element shown in Fig. 3.2 is OEGG′O′E′EO. Total power consumed within the element is the sum of power losses due to plastic deformation (φ_i), the velocity discontinuities at entry (φ_e) and outlet (φ_0) of the die, and the friction power loss along the interface between the material and the die (φ_f). The predicted total power obtained through the present velocity field would be higher (if no other redundant power losses are present) than the power actually consumed. Each power in the power element is computed numerically using velocity, strain rate components, the generalized yield stress of the material and the given friction condition. The volume and surface integration (eqns. 1.23, 1.31, 1.33 and 1.34) are carried out numerically using ten point Gauss Quadrature rule [William, et al. 1996] after extracting the necessary data from the geometry of die profile and the cross-section of the given component to be extruded.

Let $\bar{\epsilon}$ and $\bar{\sigma}$ be generalized yield strain and generalized yield stress for the given strain hardening material without consideration of the redundant work factor, and let σ_0 be the yield stress of the given material without considering strain hardening effects. Then, various powers required for the calculation of total power (φ_T) are calculated as shown below.

(a) Internal Power of Deformation

By considering an element of volume *dv* in the deformation zone subjected to a stress system σ_{ij} which causes strain rates $\in_{ij}$, the incremental power of deformation ($d\varphi_i$) can be expressed as

$$d\varphi_i = \sigma'_{ij} \, \dot{\in}_{ij} \, dv \tag{1.21}$$

The total power of deformation can be obtained by integrating $d\varphi_I$ over the entire volume of the deformation zone. Thus,

$$\varphi_i = \int_{\Omega} \sigma'_{ij} \, \dot{\in}_{ij} \, dv = \int_{\Omega} \overline{\sigma} \, \dot{\overline{\in}}_{ij} \, dv \tag{1.22}$$

The above equation in expanded form can be written as

$$\varphi_i = \frac{2}{\sqrt{3}} \overline{\sigma} \int_0^L \int_0^\phi \int_0^{R_0} \left[\frac{1}{2} . \dot{\in}_{ij} \, \dot{\in}_{ij} \right]^{1/2} |\det J| \, dn \, d\phi \, dz. \tag{1.23}$$

(b) Frictional Power

If the frictional resistance of the material along the total-work interface is τ and the slip velocity (or the tangential velocity discontinuity) along the interface is ΔV_t, then the incremental frictional power at the interface can be expressed as

$$d\varphi_f = \tau |\Delta V_t| d_s \tag{1.24}$$

where d_s is an elemental surface area. The total frictional power can be obtained by integrating the above equation along the total interface length. Thus,

$$\varphi_f = \int_s \tau |\Delta V_t| d_s \tag{1.25}$$

Here s is the area of the die-work piece interface.

In the present work, the frictional resistance on the interface is assumed to be a constant times the yield shear stress of the material $(\overline{\sigma}/\sqrt{3})$, i.e. $\dfrac{m\overline{\sigma}}{\sqrt{3}}$, where m is friction factor whose value is chosen on the basis of die-work piece interface and the lubrication conditions. The friction factor which varies from zero for frictionless condition to unity for sticking friction condition. In the present analysis friction factor is assumed to be independent of slip.

Figure 1.3 shows the relationship between the die surface and the projected surface for frictional power calculations. A small unit square element s_1 on the die surface is selected. Let $\propto$ be the maximum angle of inclination of the element (s_1) of the die surface with respect to the projected surface on the x-z plane. This angle ($\propto$) is obtained from the geometry of the die by knowing angle γ produced by the direction of a streamline (say EE′) and angle δ created by the position of this streamline. From eqn. (1.16), at the die surface,

$$E_1' = (x_1, y_1, L) \quad E_2' = (x_2, y_2, L)$$

$$E_3' = (x_3, y_3, L) \quad E_4' = (x_4, y_4, L)$$

$$E_5' = (x_5, y_5, L) \quad E_6' = (x_6, y_6, L)$$

$$E_7' = (x_7, y_7, L) \quad E_g' = (x_8, y_8, L)$$

$$(x_2, y_2, L) = (na_2 \sin\phi / R_0, n a_2 \cos\phi / R_0, L)$$

$$E = (R_0 \sin\phi, \ na_2 \cos\phi / R_0, 0)$$
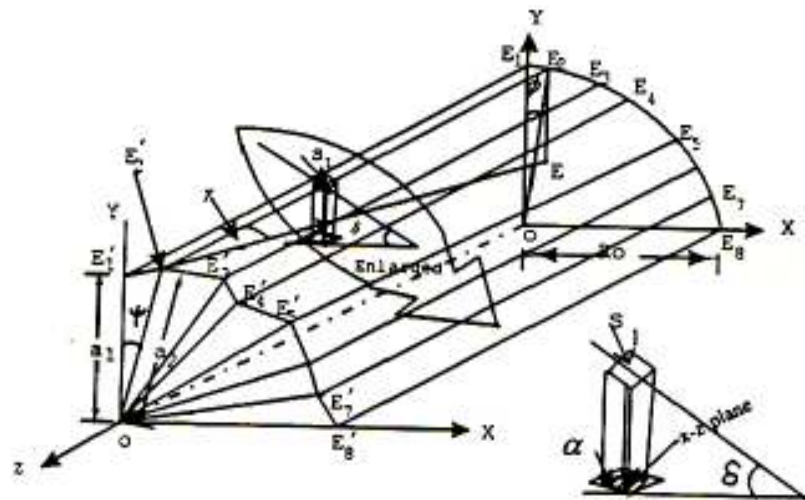
$$E_2 = (R_0 \sin\phi, \ R_0 \cos\phi, \ 0)$$

Figure 1.3: Die surface and projected surface for frictional power calculations.

$$\frac{dy}{dz} = R_0 \left(\frac{a_1}{R_0} \cos\psi - \cos\phi \right) f'; \qquad \frac{dy}{dz} = \tan\gamma \tag{1.26}$$

$$\frac{dy}{d\phi} = -R_0 \sin\phi + R_0 \sin\phi \, f \tag{1.27}$$

$$\frac{dx}{d\phi} = R_0 \cos\phi + R_0 \left(C \frac{a_1}{R_0} - \cos\phi \right) f \tag{1.28}$$

Therefore,

$$\frac{dy}{dx} = \frac{(dy/d\phi)}{(dx/d\phi)} ; \qquad \frac{dy}{dx} = \tan\delta \tag{1.29}$$

The length of diagonal (ll) of the small unit square element on the die surface is found as $ll = \sqrt{(\cos\delta)^2 + (\cos\gamma)^2}$. Angles γ and δ can be found from eqns. (1.26) and (1.29). Therefore, angle $\propto$, which is subtended by ll with the x-y plane is found as

$$\cos\alpha = \frac{ll}{\sqrt{2}}$$

On the basis of eqn. (1.25), frictional power for the considered element is obtained from the above as

$$\varphi_f = \frac{m\overline{\sigma}}{\sqrt{3}} \int_0^L \int_0^\phi \left[V_x^2 + V_y^2 + V_z^2 \right]_{n=R_0}^{1/2} \frac{1}{\cos\alpha} \frac{\partial(x,z)}{\partial(\phi,z)} \, d\phi \, dz \tag{1.31}$$

(c) Shear Power

In case the die profile has non-zero slope at the entry and exit sections, there will be shear losses due to velocity discontinuity. These planes of discontinuity can be called as the planes of sudden shear. The power dissipated along these surfaces can be calculated by employing the yield shear stress as the material resistance. Thus, the shear power can be expressed as

$$\varphi_s = \int_s \frac{\overline{\sigma}}{\sqrt{3}} |\Delta V_t| \, ds \tag{1.32}$$

Where ΔV_t is the tangential velocity discontinuity along the d_s and s is the area over which integration has to be carried out. Using eqn. (1.32) the shear power at entry (φ_e) and exit (φ_0) side are obtained as:

$$\varphi_e = \frac{\sigma_0}{\sqrt{3}} \int\limits_0^{\phi_m} \int\limits_0^{R_0} \left[V_x^2 + V_y^2\right]_{z=0}^{1/2} n \, dn \, d\phi \qquad (1.33)$$

$$\varphi_0 = \frac{\sigma_0}{\sqrt{3}} \int\limits_0^{\phi_m} \int\limits_0^{R_0} \left[V_x^2 + V_y^2\right]_{z=L}^{1/2} n \cdot C \frac{a_1^2}{R_0^2} \cdot dn \, d\phi \qquad (1.34)$$

(d) Total Power and Average Extrusion Pressure

The total power (φ_T) is the sum of its constituents including the redundant powers. Therefore, the total power (φ_T) is given as

$$\varphi_T = \varphi_i + \varphi_e + \varphi_0 + \varphi_f \qquad (1.35)$$

Once the total power (φ_T) consumed during extrusion is obtained, the upper limit to the average pressure (P_{ave}) for extrusion is found as

$$P_{ave} = \frac{\varphi_T}{\pi R_0^2 V_0} \qquad (1.36)$$

The average pressure (P_{ave}) can be converted to relative forming stress (R_S) as

$$R_s = \frac{P_{ave}}{\sigma_0} \qquad (1.37)$$

where σ_0 is the effective stress at zero hardening condition.

Analysis for Die Arrangement

Two die arrangements, square and streamlined are shown in Figure 1.4 and Figure 1.5. In the square die arrangement, the feedstock is first reduced in the chamber and in the die with round or conical corners. This includes the formation of dead metal zone and, therefore, its effect on total power consumption cannot be neglected. In streamline arrangement, there is no reduction in the abutment chamber and total reduction takes place in the die which has a pre-defined profile. Since 3rd order die profile consumes minimum power, a streamlined die profile is chosen. These two arrangements are taken to select a better option for die arrangement that consumes minimum power.

Square Die Arrangement (Figure 1.4)

For this arrangement, the dead metal zone boundary is modelled as a third order profile under sticking friction conditions (Fig. 1.4). Zone I in the abutment chamber corresponds to dead metal and zone II corresponds to the die. Since in the dead metal zone, material shears along a definite profile, sticking friction (m = 1) occurs along the dead metal zone interface.
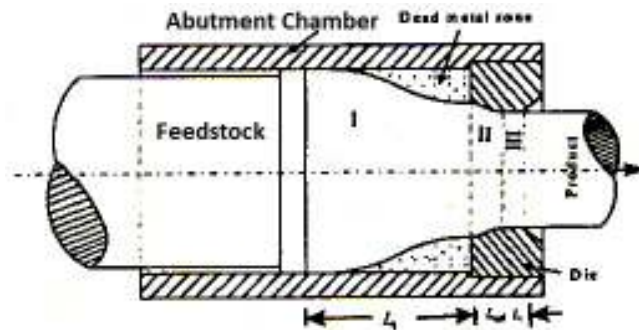
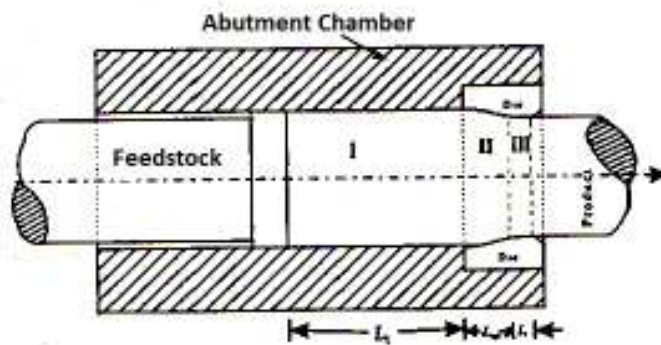Figure 1.4: **Extrusion through square die arrangement.**

Figure 1.5: **Extrusion through streamlined die arrangement.**

Total Power Losses in Die

This include the internal deformation power, the frictional power on die-workpiece interface and the discontinuity power. The total power is obtained through summation of individual powers at optimal die length (L_{opt}) . The total power in the die at optimal conditions can therefore, be evaluated as

$Pdie = (Pdiefri + Pdie_{defo} + Pdie_{disc})$

This power is calculated as

$$Pland_{fri} = m_1(\overline{\sigma}/\sqrt{3})L_1 P_1 V_{end2} 10^{-3} \text{ (Watts)} \qquad (1.38)$$

where V_{end2} is the average velocity of the extrudate in die land region, $\overline{\sigma}$ is the flow stress of material after strain hardening at the end of die exit, P_1 is the perimeter of extruded product and L_1 is taken as the one seventh of length L_{opt}.

Total power (P_{sq}) in a square die arrangement can therefore be evaluated as

$$P_{sq} = P_{dead} + P_{die} + Pcont_{fri} + Pland_{fri} \qquad (1.39)$$

Streamlined Die Arrangement (Figure 1.5)

For this arrangement (Fig. 1.5), there is no reduction in the abutment chamber. Zone I in the abutment chamber corresponds to power loss due to friction only. Zone II corresponds to the die, where all reduction takes place through a pre-defined die profile (streamlined). Since there is no dead metal zone in streamlined dies, total power can be evaluated as

$$P_{st} = P_{die} + Pabutment_{fri} + Pland_{fri} \qquad (1.40)$$

where powers P_{die} and $Pabutment_{fri}$ are found in the same way as in eqns (1.38) and (1.39). The power, $Pland_{fri}$ is found as

$$Pabutment_{fri} = (2\pi)m_c(\sigma_0/\sqrt{3})L_t R_0 V_0 10^{-3} \text{ (Watts)} \qquad (1.41)$$

with $L_t = L_0 - V_0 t$; $t_{pass} = 0.8 (L_0/V_0)$ and $t = 0.5 t_{pass}$, where L_t is the length of feedstock in the abutment chamber for average time t, and t_{pass} is the time taken by 80% of the feedstock to pass through the abutment chamber during deformation with velocity V_0.

Total powers obtained from eqns. (5.5) and (5.6) are applicable to non-re-entry component shapes. For re-entry components, the total power is found by

adding the individual powers of the proposed non re-entry shapes to the re-entry component. For re-entry component shapes also the streamlined die arrangement is found to be a better arrangement.

Die Profiles

The shape of each profile is chosen to satisfy the reduction requirements with the die length (L) as the only variable to be optimized. In certain cases, it is restricted by constraints of slope or curvature at a particular cross-section. In the present work, the following six die shapes have been considered. The die shape function $f(x)$ for these dies are given below.

S. No.	Die profile	Function $f(x)$
1	3rd order polynomial (streamlined)	$f(x) = 3\left(\dfrac{z}{L}\right)^2 - 2\left(\dfrac{z}{L}\right)^3$
2	4th order polynomial (streamlined)	$f(x) = 3\left(\dfrac{z}{L}\right)^3 - 2\left(\dfrac{z}{L}\right)^4$
3	5th order polynomial (streamlined)	$f(x) = 3\left(\dfrac{z}{L}\right)^4 - 2\left(\dfrac{z}{L}\right)^5$
4	Cosine die (streamlined)	$f(x) = 0.5\left[1 - \cos\left(\dfrac{\pi.z}{L}\right)\right]$
5	Elliptical die	$f(x) = 2\left(\dfrac{z}{L}\right) - \left(\dfrac{z}{L}\right)^2$
6	Conical die	$f(x) = \left(\dfrac{z}{L}\right)$

APPENDIX 2
RESPONSE SURFACE METHODOLOGY, ARTIFICIAL NEURAL NETWORK & GENETIC ALGORITHM

Response Surface Methodology (RSM)

Response surface methodology (RSM) is a collection of mathematical and statistical techniques for empirical model building. By careful design of experiments, the objective is to optimize a response (output variable) which is influenced by several independent variables (input variables). An experiment is a series of tests, called runs, in which changes are made in the input variables in order to identify the reasons for changes in the output response. Originally, RSM was developed to model experimental responses (Box and Draper, 1987), and then migrated into the modelling of numerical experiments. The difference is in the type of error generated by the response. In physical experiments, inaccuracy can be due, for example, to measurement errors while, in computer experiments, numerical noise is a result of incomplete convergence of iterative processes, round-off errors or the discrete representation of continuous physical phenomena (Giunta et al., 1996; van Campen et al., 1990, Toropov et al., 1996). In RSM, the errors are assumed to be random.

Plackette-Burman Design (PBD)

Plackett-Burman experimental design is used to identify the most important factors early in the experimentation phase when complete knowledge about the system is usually unavailable. Developed in 1946 by statisticians Robin L. Plackett and J.P. Burman, it is an efficient screening method to identify the active factors using as few experimental runs as possible.

In Plackett-Burman designs, main effects have a complicated confounding relationship with two-factor interactions. Therefore, these designs should be used to study main effects when it can be assumed that two-way interactions are negligible.

In practical use, two-level full or fractional factorial designs, and Plackett-Burman designs are often used to screen for the important factors that influence process output measures or product quality. These designs are useful for fitting first-order models (which detect linear effects) and can provide information on the existence of second-order effects (curvature) when the design includes center points.

Neural Networks

Neural network are motivated by the functioning of brain, which consists of a number of neurons. The network in the brain is called biological neural network, whereas we build artificial neural networks for solving physical problems. The artificial neural network (ANN) may be very different from a biological neural network. Neural networks are systems which can acquire, store and utilize knowledge gained from experience. Neural network techniques have been found capable of learning from a dataset to describe the non-linear and interaction effects with great success [Holland et al., (1975)]

As a very simple example of how a neural network can be used, consider dependent variable z related to independent variables x and y in the following manner:

$$z = x^2 + y^2 \qquad\qquad (2.1)$$

If just provided a few datasets in the form of triplet (x, y, z), the neural network must be able to understand that the function is of the form given in Equation (2.1). The important point is that too many exemplars should not be required. The data by which the neural network understand the relation between the variables called training data. After the network has been trained based on the training data it has to be tested with a few data called testing data.

Biological Neural Networks

The brain consists of a densely interconnected set of nerve cells, or information processing units, called neurons. The human brain incorporates near about 11^{10} neurons and 10^{14} connections through synapses between them. Although neurons has a very simple structure, a combination of such elements constitute tremendous processing power. As shown in Figure 2.1, a neuron consists of a c body, soma, a number of fibers

called dendrites, and a single long fiber called axon. Dendrites form a very fine bush of thin fibers around the neuron's. Dendrites receive information from neurons through axons (long fibers) that seen as transmission lines. An axon is a long cylindrical connection that carries impulses from the neuron. At the end part of an axon, various branches terminates the surface of other neurons or on the dendrites. The axon-dendrite contact organ called a synapse, through which the neuron introduces its signal to the neighbor neuron. Signals are propagated from one neuron to another by component electrochemical reactions. Signals travel in the axon in the form of electrical impulses. Synapses convert the electrical single into chemical ones. Chemical substances released from the synapses cause a change in the electrical potential the cell body. When the potential of the cell body reaches its threshold, electrical pulse, action potential, is generated. This pulse is transmitted through axon to reach the other synapses, causing them to increase or decrease the potential of cell bodies. Usually, each neuron has one axon to transmit the signal thousands of synapses to receive the single from the other neurons. Generation electrical impulse by the cell body is called firing of the neuron. If the income impulses help in firing of a neuron, they are called excitatory impulses. If t hinder the process of firing, they are called inhibitory.

In response to the stimulation pattern, neurons demonstrate long-term chain in the strength of their connections. Neurons can also form new connections other neurons. Even entire collections of neurons may sometimes migrate from place to another. These mechanisms form the basis for learning in the brain. T phenomenon is called plasticity. The plasticity diminishes with age. It has been found that a typical human brain loses about 2-5% of its total neurons by the time it reaches 50 years of age.

A human brain can be considered as a highly complex, non-linear and parallel information-processing system. Information is stored and processed in a neural network simultaneously throughout the whole network, rather than at specific locations. In other words, in neural networks, both data and its processing are global rather than local. Owing to the plasticity of the network, connections between neurons leading to the 'right judgment' are strengthened while those leading to the 'wrong judgment' become weak. As a result, neural networks have the ability to learn through the experience. Learning is a fundamental and essential characteristic of biological neural networks. The ease and

naturalness with which they can learn motivated us to emulate a biological neural network in a computer. However, the types of artificial neural network, which are described in this chapter, are highly simplified versions of actual biological network [Jang et al., (2002)].
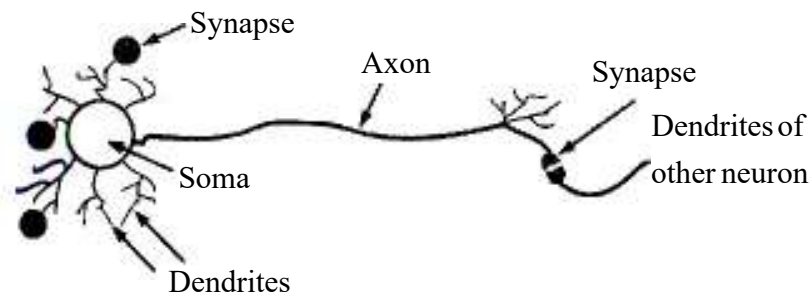

Figure 2.1: A typical biological neuron

Perceptron: The Learning Machine

In the previous subsection, a model of a single neuron has been presented. The neuron can behave in a particular way depending on its weights and bias. However, it must have the ability to learn through exemplar in order to emulate the behavior of a biological system. In 1958, Rosenblatt introduced the first learning machine, discrete (binary) perceptron. The perceptron will be as shown in Figure 2.2 with the ability to adjust its weights and bias with supplied training data. The learning method in which the data in the form of input and output is supplied and the network is trained to minimize the error is reduced by making small adjustments in the weights to reduce the difference between the predicted and the desired output of the perceptron. The initial weights are randomly assigned and then updated to obtain the output consistent with the training examples. For a perceptron, the process of weight updating is simple. If at iteration p, the predicted output is $o(p)$ and the desired output (target) is $d(p)$, then the error is given by

$$e(p) = d(p) - o(p) \text{ where } p = 1, 2, 3\ldots\ldots \quad (2.2)$$

At each iteration a fresh training data is presented to the perceptron. If the error $e(p)$, is positive, we need to increase the perceptron's output $o(p)$, but if it is negative, we need to decrease $o(p)$. Taking into account that each perceptron input contributes $x_i(p) \times w_i(p)$ to the total input $X(p)$, we find that if input value $x_i(p)$ is positive, an increase in its

weight $w_i(p)$ tends to increase perceptron output $o(p)$. On the other hand, if x_i (p) is negative, an increase in $w_i(p)$ tends to decrease $o(p)$. Thus, the following perceptron learning rule can be established:

$$w_i\,(p+1) = w_i\,(p) + \alpha x_i\,(p) \times e\,(p)\,, \qquad (2.3)$$

Where α is the learning rate.

Multi-Layer Perceptron Neural Networks

A multi-layer perceptron (MLP) is a feedforward neural network with one or more hidden layers. A feedforward network has a sequence of layers consisting of a number of neurons in each layer. The output of neurons of one layer becomes input to neurons in the succeeding layer. The output of neurons of one layer becomes input to neurons in the succeeding layer. Typically a network consists of an input layer consisting of neurons corresponding to input variables, at least one middle or hidden layer of computational neurons, and an output layer of computational neurons. The input signals are propagated in a forward direction on a layer-by layer basis. A multi-layer perceptron with one hidden layer is shown is Figure 2.2. The first layer, called an input layer, receives data from the outside world. The last layer is the output layer, which sends information out to users. Layers that lie between the input and output layers are called hidden layers and have no direct contact with the environment. Their presence is needed in order to provide complexity to network architecture for modeling non-linear functional relationship. After choosing the network architecture, the network is trained by providing data in the form of several input-output pairs. During the training process, the network adjusts its weights to minimize the error between the predicted and desired outputs.

The most common algorithm the error between the predicted and desired outputs. Algorithm. Here, the training process involves two passes. In the forward pass, the input signals propagate from the network input to output. In the reverse pass, the calculated error signals propagate backwards through the network where they are used to adjust the weights. The error signal is the mean squared error given by

$$E = \frac{1}{2}\sum_{k=1}^{K}(d_k - o_k)^2\,, \qquad (2.4)$$

Where d_k is the desired k-th output and o_k is the predicted k-th output of the network. K is the number of neurons in the output layer.

Any efficient optimization method can be used for minimizing the error through weight adjustment. The calculation of the output is carried out layer by target value of each output neuron is available to guide the adjustment of the associated weights. Next, the weights of the middle layers are adjusted. Since the middle layers have no target values; errors of the succeeding layers. After proper transformations, are propagated back through the network, layer after proper transformations, are propagated back through the network, layer by layer. Hence, this algorithm is termed as back propagation algorithm. The trained neural network has to be tested by supplying testing data. If the testing error is much more compared to the training error, the network is said to over-fit the data. A properly fitted ne
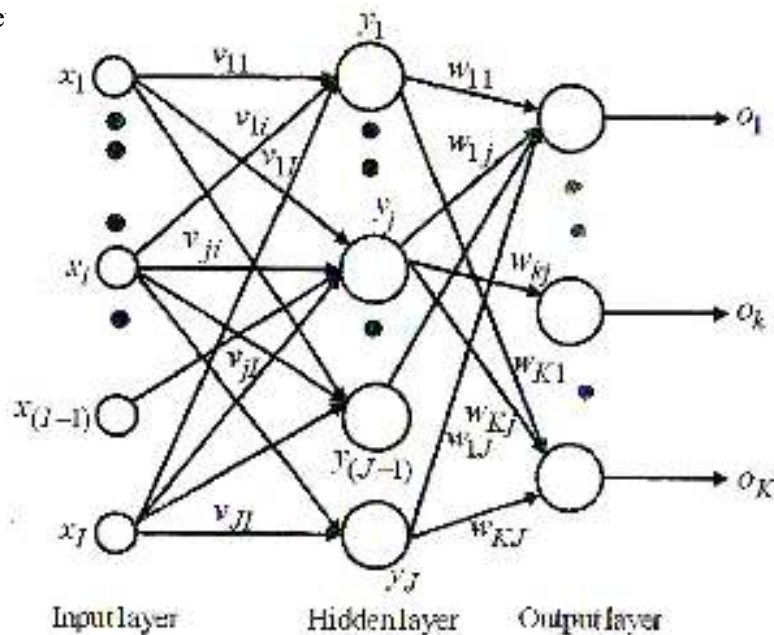
Figure 2.2: A multi-layer perceptron with one hidden layer

Radial Basis Function Neural Network

The supervised training of the neural network can be viewed as a curve fitting process. The network is presented with training pairs, each consisting of a vector from an input space and a vector from the output space. Through a defined learning algorithm, the network perform the adjustments of its weights so that the error between the actual and

desired outputs is minimized relative to some optimization criterion. The trained network performs the interpolation in the output vector space, which is referred to as the generalization property. In this subsection, we describe a radial basis function neural network as an alternative to multi-layer perceptron neural network to carry out this task.

The radial basis function (RBF) network consists of three layers: an input layer, a single layer of non-linear processing neurons, and an output layer. Figure 8.6 shows a typical network. For a network having K neurons in the output layers and J neurons in the hidden layer, the output of RBF is calculated according to

$$o_i = f_i(x) = \sum_{j=1}^{J} w_{ij} \phi_j \left(\left\| x - x_j^c \right\|_2 \right) \text{where} i = 1, 2 \ldots \ldots K, \quad (2.5)$$

where x is the input vector, ϕ_j (.) is function from set of all positive real number to set of real numbers, $\left\| . \right\|_2$ denotes the Euclidean norm, w_{ij} are the weights in the output layer, and x_j^c are the RBF centers in the input vector space. For brevity, we will use $\left\| . \right\|$ to mean Euclidean norm, omitting subscript 2. For each neuron in the hidden layer, Euclidean distances between its associated center and the input to the network are computed. The output of the neuron in a hidden layer is a non-linear function of the distance. The most common function is Gaussian function given by

$$\phi_j(x) = exp \left\{ - \frac{\left\| x - x_j^c \right\|^2}{2\sigma_j^2} \right\}, \quad (2.6)$$

where σ_j^2 is called the variance, which controls the spread of the distribution about the center.

Unsupervised Learning

The neural network discussed in the previous sections used supervised learning algorithms, which are based on error corrections rules. In these algorithms, an error value is generated from the actual response of the network and the desired response. After that, the weights are modified such that the error is gradually reduced. In unsupervised learning, there is no feedback from the environment for assessing the correctness of the

mapping. In other words, there is no "teacher". Instead the network must be able to discover by itself any categories, patterns, or features possibly present in the data. Network that are able to infer pattern relationship without being supervised are also called self-organizing.

There are many unsupervised learning rules. One rule was proposed by Hebb in his seminal work, "The organization of Behavior". This is called the Hebbian learning rule. It makes the weight strength proportional to the product of the firing rates of the two interconnected neurons. That is, when two connected neurons fire at the same time and repeatedly, the synapse's strength is increased.

Competitive learning is an unsupervised learning procedure in which the neurons of a network learn to recognize clusters of similar input vectors. The network detects regularities and corrections among the input vectors and adapts the future response of the units to similar inputs. In competitive networks, output units compete among themselves for activation. The simplest competitive learning network consists of a single layer of output neurons to which all inputs are connected. All the units are presented with given input vectors but only one output neuron is activated at any given time: the so-called winner neuron.

Genetic Algorithms

There are a number of evolutionary algorithms, which mimic natural evolutionary principles for optimizing. Among them, genetic algorithms are very powerful evolutionary optimization techniques, which do not required the derivatives of the objective and constraint functions. These are so named because they follow the principles of natural genetics. Professor John Holland of the University of Michigan, Ann Arbor, first envisaged the concept of these algorithms. Now, there are many variants of these algorithms. We will briefly describe two of them *i.e.*, binary-coded and real-coded genetic algorithms. There are a number of advantages of using genetic algorithms (GAs) [Goldberg et al., (1989)]:

- GAs are parallel-search procedures that can be implemented on parallel-processing machines for very fast computations.

- GAs are applicable to both continuous and discrete design variable optimization problems.

- They are suitable for combinatorial optimization problems, where the solution space contains finite set of points.

- GAs are stochastic and are less likely to get trapped in local minima, which inevitably are present in most of the practical applications.

- GAs are very suitable for solving multi-objective problems.

Binary Coded Genetic Algorithms

These are the original genetic algorithms. In this book, we will refer a binary coded genetic algorithm as BGA and a real coded genetic algorithm as RGA. The term GA will be used as a general term to mean both types of genetic algorithms. In BGA, the design variables of the optimization problem are coded in binary form. Thus, instead of operating on real values of design variables, we operate on the binary values. Thus, a solution point is represented by a string (chromosome) consisting of '0's and '1's. Each '0' and '1' value is called a bit and is analogous to a gene. The mapping between the

binary and real form can be easily established. Suppose the i-th variable is represented by a sub-string S_i, then its real value is given by

$$x_i = x_i^L + \frac{x_i^U - x_i^L}{2^{l_i} - 1} \text{ (Decoded (decimal) value of } S_i),\tag{2.2.1}$$

where x_i^L and x_i^U are the lower and upper bounds of the variable and l_i is the length of the string. The higher is the length of the string, the higher is the precision.

Reproduction

This is the first operator applied on a population. In reproduction, good strings in a population are assigned a large number of copies. The reproduction can be carried out in a number of ways. In the tournament selection, tournaments are played between two solutions and the winning solution is taken. By tournament playing we mean that two solutions are compared and the solutions are compared and the solution having the better fitness is chosen. Each solution participates in exactly two tournaments in a random manner. Thus, the best solution gets two copies in the population and the worst having lost both the tournaments gets eliminated. Other solution may get zero, one or two copies in the population. Figure 2.3 illustrates the procedure pictorially. The population consists of four members. It is assumed that the fitness value of each member is proportional to his height. Four tournaments are played and the taller member wins. In this way, we get two copies each of the tallest and second tallest. Note that other possibilities also exist depending on how the teams are formed. Thus, probability plays a role here.

In proportionate selection, copies proportional to fitness values are taken. Supposing the fitness values is 125. Dividing the fitness values by this number, we get the probabilities of survival of different members. In this case, the probabilities are 0.2, 0.4, 0.08 and 0.32. Expected number of copies are found by multiplying these probabilities with the size of the population, in this case 4. Thus, the members are expected to have 0.8, 1.6, 0.32 and 1.28 copies. This means that if the reproduction operator is carried out a large of times, on an average these will be the number of copies. However, in any single operation a particular member may get 0, 1, 2, 3 or 4 copies. For achieving this operation in a computer, the following procedure may be adopted [Deb et al., (2003)]:
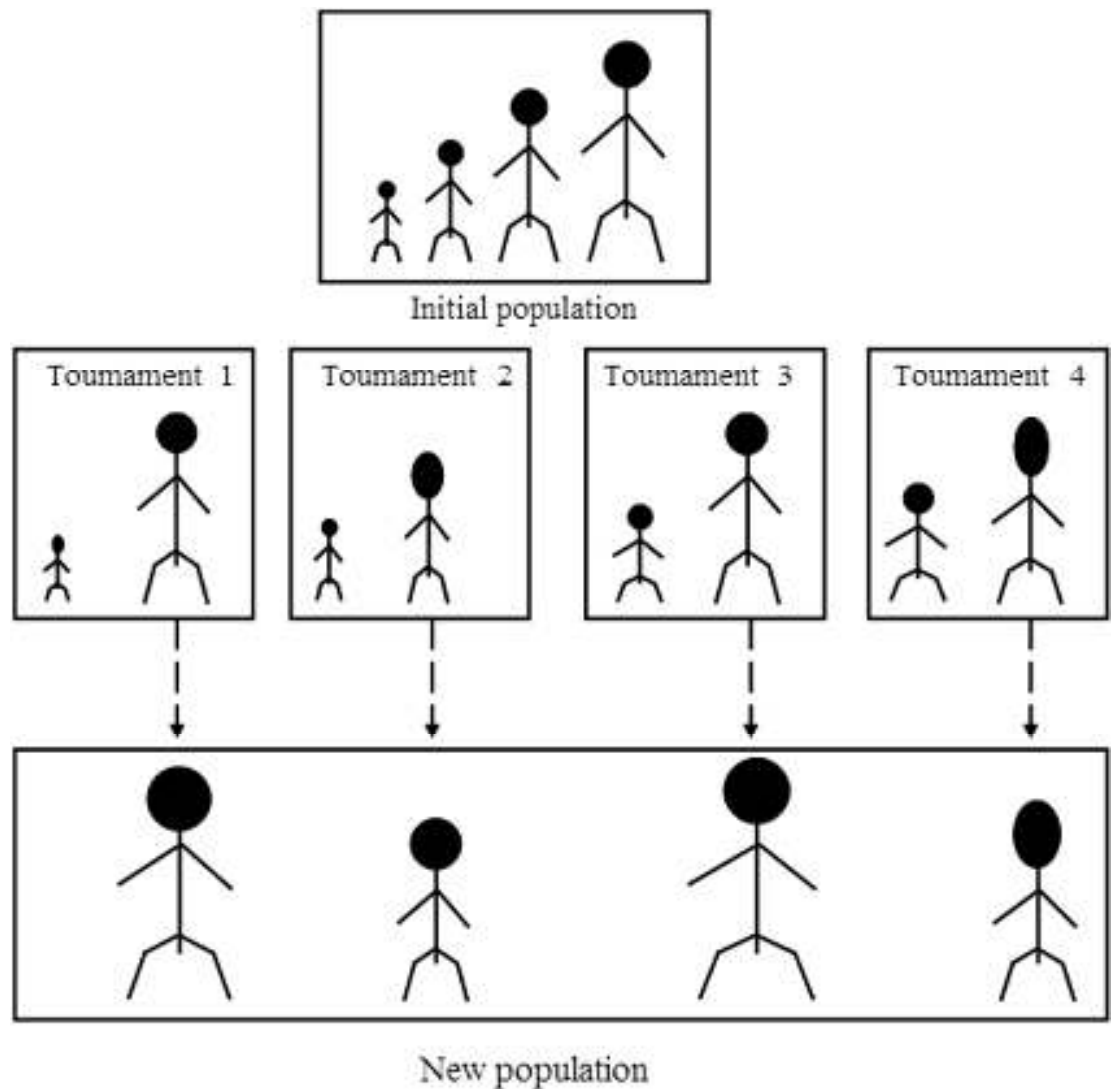
Figure 2.3: Reproduction using tournament selection

- We make ranges proportional to the probabilities between 0 and 1. In our case, the ranges are $0 - 0.2$, $0.2 - 0.6$, $0.6 - 0.68$ and $0.68 - 1.0$.

- Generate random numbers equal to the number of members in the population. In whatever range a particular number falls, the corresponding chromosome is selected.

This method of selection is called roulette wheel selection (RWS), because the same operation can be achieved mechanically by spinning a wheel a number of times. The wheel (shown in Figure 2.4) is divided into divisions equal to

population size, where the size of each division is proportional to the fitness of the corresponding member. The wheel is spun and is allowed to stop. Then the member whose division stops before a fixed pointer is selected.
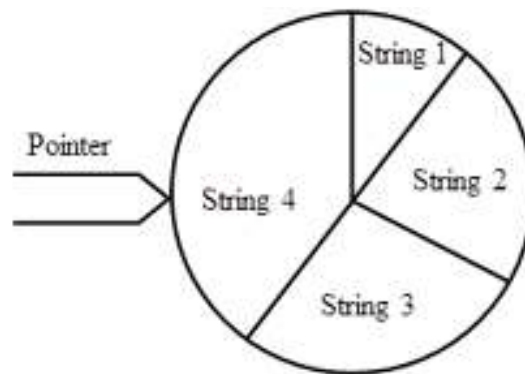
Figure 2.4: A Roulette Wheel

The proportionate selection operator has scaling problem. If the fitness value of one member is more, the member gets selected quite often. Similarly, if the fitness values of all members are more or less the same, all members have equal probability of getting selected. The tournament selection does not have this ranking problem. The scaling difficulty can be eliminated by using a ranking selection operator. In this method, solutions are sorted according to their fitness values and the ranks are assigned, the worst member getting the rank 1. The proportionate selection is then applied based on these ranks.

Crossover

In crossover operation, new chromosomes are created by exchanging the information between two chromosomes. To accomplish this, the following procedure is adopted. If the population size is N, N/2 pairs are formed at random. Two chromosomes (strings) in each pair are called parents. Taking each pair at a time, a random crossover site is selected. Then, two off string (children) are produced by exchanging all the bits on the right side of the cross-over site. More Crossover operation is carried out with some probability. This is because, some good strings have to be preserved. If a crossover probability of p_c is chosen, then 100 p_c % of the strings are used for cross-over and the remaining strings are

copied as they are to the next population. A common practice is to choose about ¾-th string for the crossover.

 Mutation

Mutation changes the bits of the chromosomes with some low probability (typically 0.01) of mutation. It is needed to provide some diversity in the population. It serves the crucial role of preventing the system from getting stuck to the local optimum. Only reproduction and mutation operations do not guarantee true optimum points. Mutation can randomly create a very good chromosome. It may also create a very bad chromosomes, but it will hopefully not get transferred in the next generation.

APPENDIX 3

Finite Element Formulation (Updated Langrangian)

Let du_i, $d\varepsilon_{ij}$ and $d\sigma_{ij}$ be the components of the incremental displacement vector, the incremental linear strain tensor and the incremental Cauchy stress tensor respectively. As before, we assume that the process is isothermal. For an isothermal process, the increment du_i, $d\varepsilon_{ij}$ and $d\sigma_{ij}$ are governed by the following equations. For the sake of completeness, these equations have been reproduced below.

Governing Equations:-

(i) Incremental strain – displacement relations (Equation 3.1), six scalar equations:

$$d\varepsilon_{ij} = \frac{1}{2}(du_{i,j} + du_{j,i}). (3.1)$$

(ii) Incremental elastic-plastic stress-strain relations six scalar equations:

After Yielding:

$$d_{\sigma ij}^{0} = C_{ijkl}^{EP} d\varepsilon_{kl}, \tag{3.2}$$

Where

$$C_{ijkl}^{EP} = 2\mu \left[\frac{v}{1-2v} \delta_{ij}\delta_{kl} + \delta_{ik}\delta_{jl} - \frac{9\mu}{2} \frac{\sigma'_{ij}\sigma'_{kl}}{(H'+3\mu)\sigma^2_{eq}} \right], \tag{3.3}$$

$$\sigma_{eq} = \sigma_Y + K(\varepsilon^p_{eq})^n, \tag{3.4}$$

$$v = \frac{\lambda}{2(\lambda + \mu)}; \tag{3.5}$$

Before yielding and after unloading;

$$d_{\sigma ij}^{0} = C_{ijkl}^{E} d\varepsilon_{kl}, \tag{3.6}$$

Where

$$C_{ijkl}^{E} = \lambda\delta_{kl}\delta_{ij} + 2\mu\delta_{ik}\delta_{jl}. \tag{3.7}$$

Here, the superscript ^{0} on the stress increment in Equations 3.2, e means it is the *product of the Jaumann stress rate and the time increment* . The Jaumann stress rate is related to the Cauchy stress rate through spin tensor. As the product of spin tensor and the time increment is equal to the incremental infinitesimal rotation tensor which is given by Equation (3.8). Thus, we have

$$d^0_{\sigma_{ij}} = \overset{0}{\sigma}_{ij}\, dt,$$

(3.8)

Where

$$\overset{0}{\sigma}_{ij}\, dt = \dot{\sigma}_{ij}\, dt - (\dot{\omega}_{il}\, dt\sigma_{ij} + \sigma_{il}\, \dot{\omega}_{lj}^T\, dt) = d\sigma_{ij} - (d\omega_{il}\sigma_{ij} + \sigma_{il} d\omega_{lj}^T),$$

(3.9)

$$d\omega_{ij} = \frac{1}{2}(du_{i,j} - du_{j,i}).$$

(3.10)

(iii) Incremental equations of motion, three equations:

$$\rho da_i = \rho db_i + d\sigma_{ij,j} \, .$$

(3.11)

As decided earlier, we treat ρ as a constant. Therefore, we do not need the equation of conservation of mass. Thus, we have 15 scalar equations for 15 unknowns: (i) 3 incremental displacement components du_i, (ii) 6 incremental linear strain components $d\varepsilon_{ij}$ and (iii) 6 incremental Cauchy stress components $d\sigma_{ij}$. To solve these equations for the given material, the material properties have to be supplied: (i) density ρ, (ii) elastic properties λ and μ and (iii) the yield stress σ_Y and the hardening parameters K and n. Further, the incremental body force db_i (per unit mass) also has to be specified).

Boundary Conditions

Typical boundary conditions are as follows. As before, we denote the boundary of the domain by S.

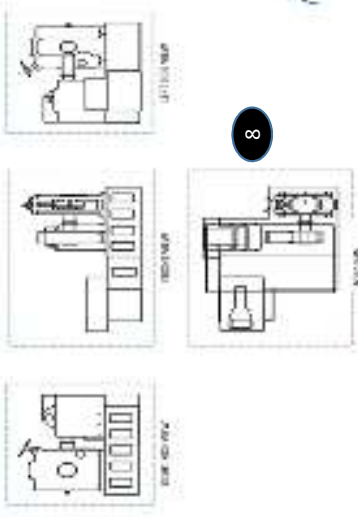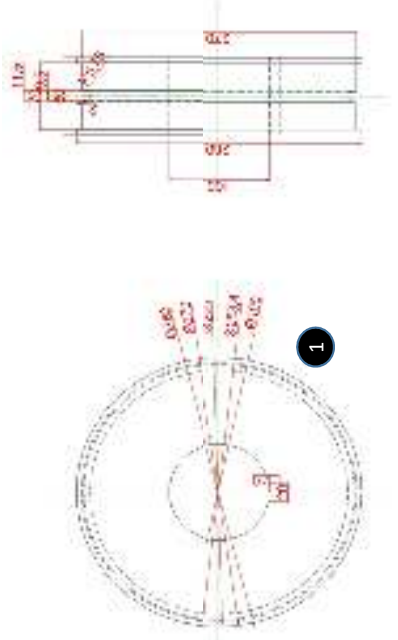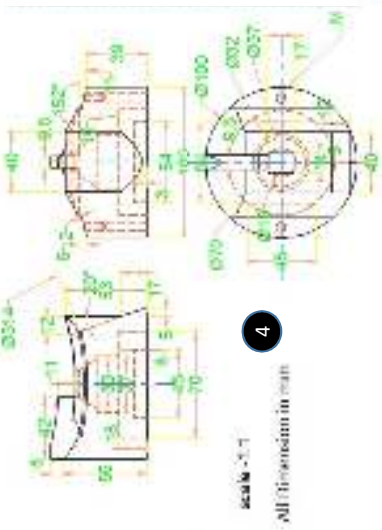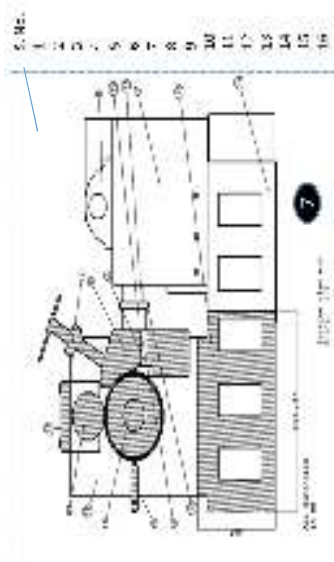(i) On a part of the boundary (S_u), an incremental displacement vector **du** is specified. Thus,

$$du_i = du_i^* \text{ on } S_u,$$

(3.12)

where du_i^* represents the specified value. This is called the *kinematic* or *displacement* boundary condition.

(ii) On the remaining part of the boundary (S_t), an incremental stress vector $dt_n = d\sigma\hat{n}$ is specified, thus,

$$(dt_n)_i \equiv d\sigma_{ij}n_j = (dt_n^*)_i \text{ On } S_t, \qquad (3.13)$$

Where $(dt_n)_i^*$ represents the specified value. This is called the *stress* or *traction* boundary condition.
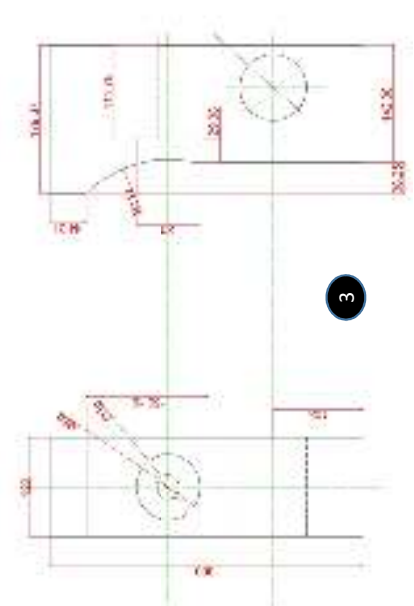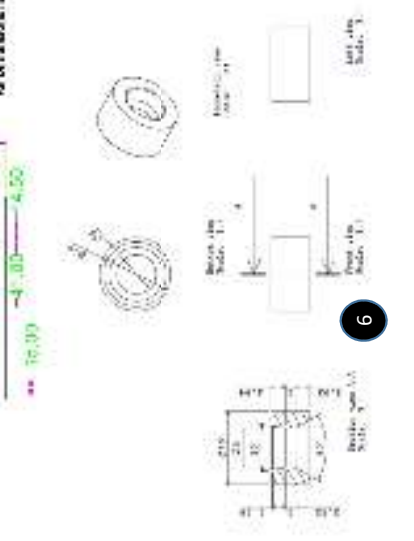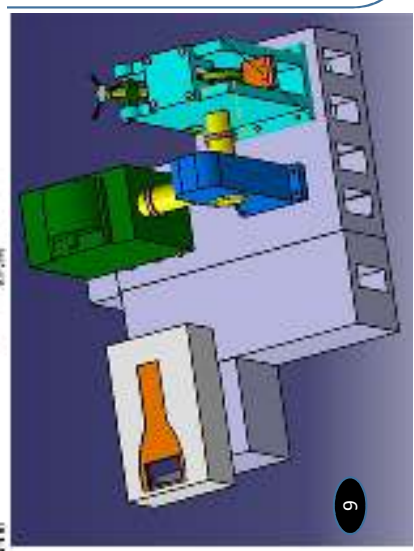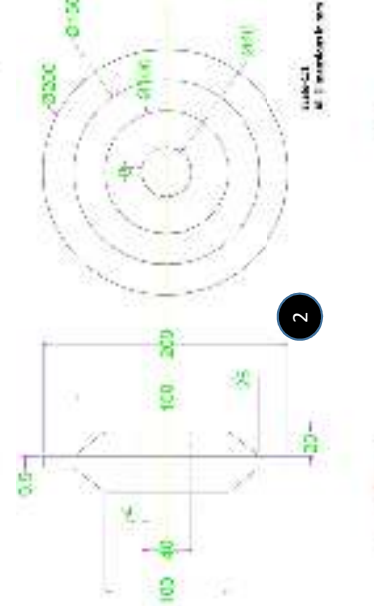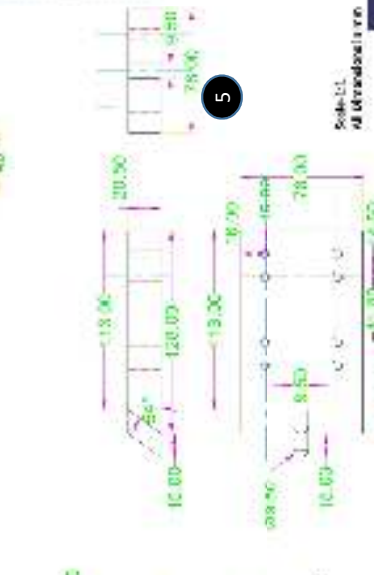
10

S. No.	Part
1	Dimple Wheel
2	Coining Wheel
3	Extrusion Shoe
4	Hammer for Closure
5	Die
6	Scraper
7	Mechanical Interrupter
8	Feedit Roller
9	Motor Pulley
10	Contact Shoe
11	Motor Shaft
12	Coupling of motor and worm shaft
13	Worm Gear
14	Motor Base
15	Coining Wheel Mounting Unit
16	Machine Frame

1. Extrusion Wheel
2. Coining Wheel
3. Extrusion Shoe
4. Die
5. Abutment Die Chamber
6. Scraper
7. Variable frequency drive
8. 3-Phase AC motor
9. Worm Gearbox
10. Heating arrangement
11. Design Developed and Fabricated Continuous Extrusion setup
12. View of Continuous Extrusion setup
13. Meshing view of Extrusion and Coining Wheel

Comparisons in Design of Continuous Extrusion elements before and after modification

S. No.	Element	Before Modification	After Modification	Remarks
1	Extrusion Wheel			Before modification, extrusion wheel groove was shallow suitable for 8 mm Aluminum feedstock. After modification, wheel groove is much deeper suitable for 9.5 mm Aluminum feedstock.
2	Coining Wheel			Before modification, coining wheel was grooved whereas after modification coining wheel is flat in design.

| No.	Name			Description
3	Extrusion Shoe			Before modification extrusion shoe has groove on its surface whereas extrusion is flat in design after modification.
4	Abutment			Abutment before modification was unable to pass the material into die cavity whereas after modification extrusion has taken place successfully.
5	Die			Die before modification was flat unable to extrude the feedstock material. After modification conical die has been developed.

6	Scraper	No Scraper	Before modification no scraper was incorporated in the setup whereas after modification scraper has been incorporated which is very essential for removal of flash formed.
7	Gearbox		Before modification reduction capacity of gearbox was low as compared to gearbox after modification.
8	Motor		Before modification the power and torque provided by electric motor was not suitable for extrusion of material whereas after modification 45 kW AC Drive motor has been found suitable for extrusion of Aluminum feedstock.

|			
9	Variable Frequency Drive	No Variable Frequency Drive		Before modification, no variable frequency drive was incorporated in the setup whereas after modification variable frequency drive of 50 HP has been incorporated suitable for variation of speed of extrusion wheel as per desire.
10	Heating arrangement	No Heating arrangement		Before modification, no heating arrangement was made for heating of die chamber which is very essential in continuous extrusion process whereas after modification suitable heating arrangement has been made.

APPENDIX 4

DRAWINGS

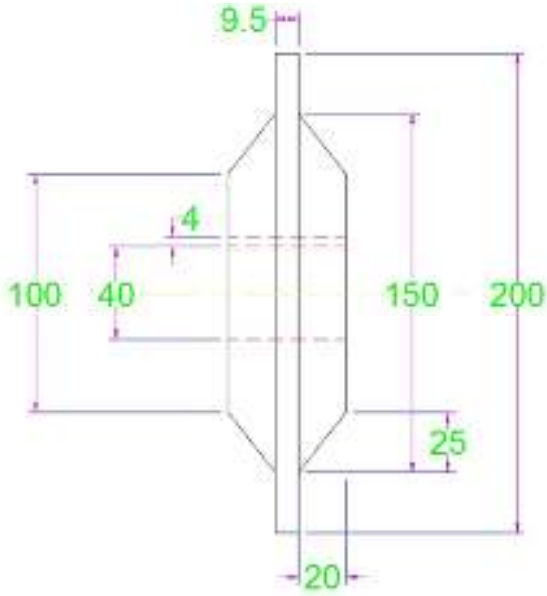
EXTRUSION WHEEL
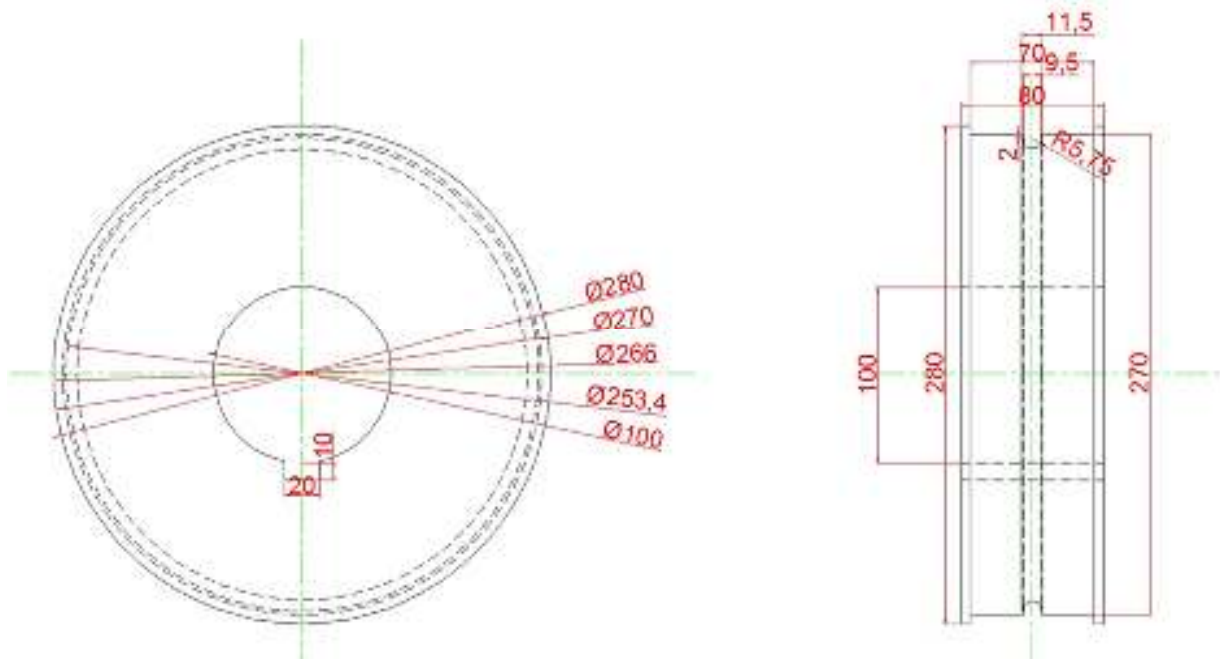
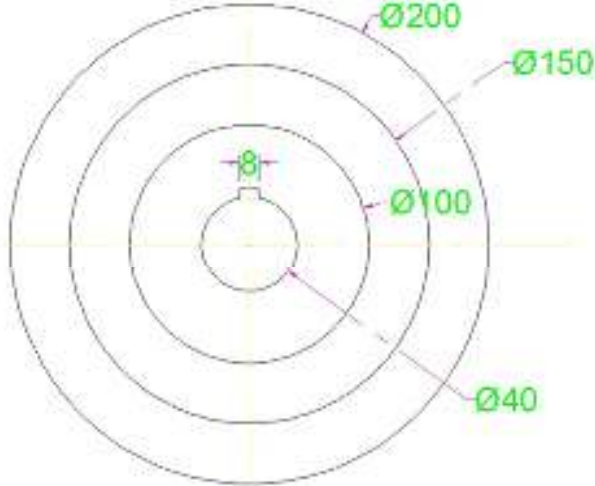
SIDE VIEW   **FRONT VIEW**

EXTRUSION SHOE
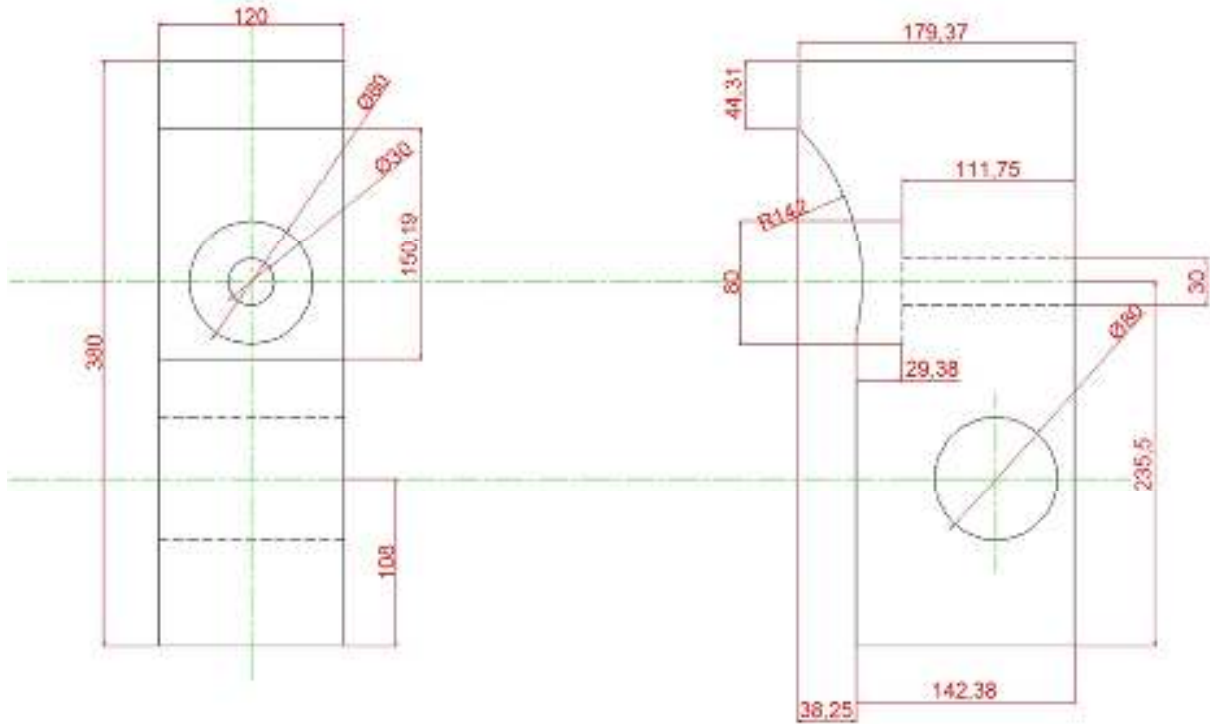
FRONT VIEW

SIDE VIEW

COINING WHEEL

FRONT VIEW

SIDE VIEW

316

SCRAPER

Scale-1:1
All Dimensions in mm

ABUTMENT DIE CHAMBER

scale -1:1

All Dimension in mm